

## Tensor network simulation of an SU(3) lattice gauge theory in 1D

Pietro Silvi,<sup>1</sup> Yannick Sauer,<sup>2</sup> Ferdinand Tschirsich,<sup>2</sup> and Simone Montangero<sup>2,3,4</sup>

<sup>1</sup>*Center for Quantum Physics, and Institute for Experimental Physics, University of Innsbruck and Institute for Quantum Optics and Quantum Information, Austrian Academy of Sciences, A-6020 Innsbruck, Austria*

<sup>2</sup>*Institute for Complex Quantum Systems and Center for Integrated Quantum Science and Technologies, Universität Ulm, D-89069 Ulm, Germany*

<sup>3</sup>*Theoretische Physik, Universität des Saarlandes, D-66123 Saarbrücken, Germany*

<sup>4</sup>*Dipartimento di Fisica e Astronomia, Università degli Studi di Padova, I-35131 Padova, Italy*



(Received 23 January 2019; published 28 October 2019)

We perform a zero temperature analysis of a non-Abelian lattice gauge model corresponding to an SU(3) Yang-Mills theory in 1 + 1D at low energies. Specifically, we characterize the model ground states via gauge-invariant matrix product states, identifying its phase diagram at finite density as a function of the matter-gauge interaction coupling, the quark filling, and their bare mass. Overall, we observe an extreme robustness of baryons: For positive free-field energy couplings, all detected phases exhibit colorless quasiparticles, a strong numerical hint that QCD does not deconfine in 1D. Additionally, we show that, having access to finite-density properties, it is possible to study the stability of composite particles, including multibaryon bound states such as the deuteron.

DOI: [10.1103/PhysRevD.100.074512](https://doi.org/10.1103/PhysRevD.100.074512)

### I. INTRODUCTION

The theory ruling the strong interactions within and among hadrons, quantum chromodynamics (QCD), is the main focus of much of the current experimental and theoretical effort in high energy physics [1]. Many of the collective phenomena arising from this theory, including the phase diagram, have yet to be fully characterized, especially at finite density [2,3]. In fact, nonperturbative numerical approaches based on lattice formulations [4–7], such as Monte Carlo simulations, suffer by the notorious sign problem for complex actions, e.g., in the presence of fermions, such as quarks, or at finite chemical potentials [8]. A promising alternative route to simulate gauge theories modeled on a lattice based on tensor network (TN) ansatz states has recently been put forward. Indeed, TNs have already shown significant capabilities, delivering quantitative predictions for lattice gauge theories in one spatial dimension [9–12]. Mostly, Abelian lattice gauge theories have been investigated [13–21], with a few non-Abelian exceptions [22–24]. Yet, to our knowledge, no further attempt at capturing the phase properties of a microscopic dynamics analogous to QCD has been made.

Here we present the TN study of a one-dimensional lattice gauge theory with SU(3) symmetry as a quantum link model [25–28], and specifically the formulation of Ref. [29]. The model involves flavorless Kogut-Susskind matter fermions [5] and SU(3) Yang-Mills gauge fields, truncated to the first nontrivial Casimir operator excitation. We investigate the equilibrium properties of this QCD-like model at finite density, at zero temperature and finite lattice

spacing  $\ell$ . We show that TN enables investigation of the confinement problem in models of increasing complexity and by means of different tools, identifying phases, order properties, and binding energies of composite particles. In particular, for zero quark bare mass, we detect a Luttinger liquid of baryons at finite nonzero charge density. Only at no charge imbalance does the theory exhibit insulating phases, one spontaneously breaking chiral symmetry at low interactions, and another forming dimers in open-boundary conditions for large interactions. Finite bare masses open energy gaps for weak interactions, resulting in insulating phases even at finite density. Finally, we show by directly evaluating the binding energy that it is more energetically favorable to form colorless baryons than colorful particles, and that in this theory the deuteron is not energetically stable.

These results foster further development of analogous modelizations in two or more dimensions, as well as the development of quantum simulation strategies [30–36], on atomic-molecular-optical platforms, capable of implementing such interesting lattice gauge physics, such as the recently proposed hybrid simulators [37–39].

### II. MODEL

We consider a lattice gauge model in one spatial dimension equipped with an SU(3) local gauge symmetry. The matter-field sublattice, labeled with sites  $\{j\}$ , hosts colorful (spinless, flavorless) Kogut-Susskind (KS) fermions [5,40]  $c_{j,a}$ , with  $\{c_{j,a}, c_{j',b}^\dagger\} = \delta_{j,j'}\delta_{a,b}$ : Odd sites

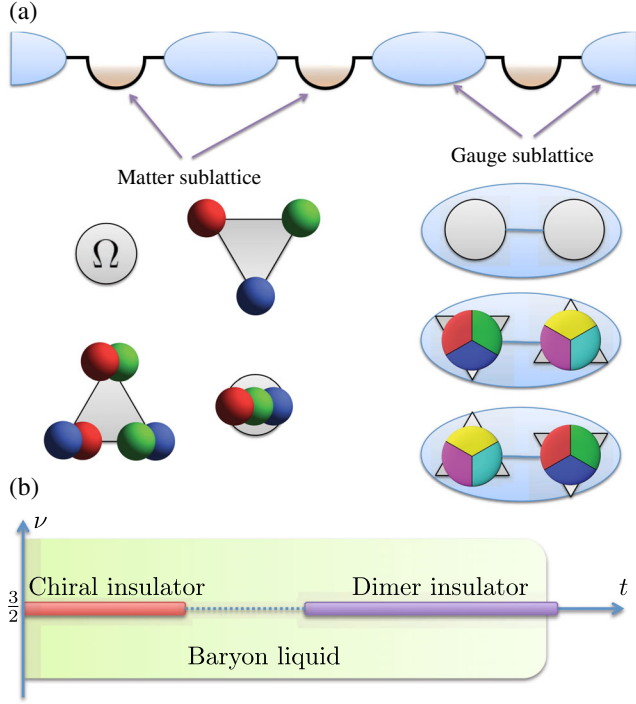


FIG. 1. (a) Schematic description of the d.o.f. KS fermions live on the matter sublattice: They represent quarks (odd sites) or antiquark holes (even sites) and have three colors ( $r, g, b$ ). Listing the eight local matter states according to the total filling highlights the corresponding SU(3) irreducible representation (irrep): The empty state is a color singlet (gray bullet), the singly filled states form a  $q$  irrep ( $\nabla$  triangle), the doubly filled states form a  $\bar{q}$  irrep ( $\Delta$  triangle), and the triply filled state form another color singlet. The truncated gluon field space we consider includes 19 states: one singlet-singlet state, nine  $q \otimes \bar{q}$  states, and nine  $\bar{q} \otimes q$  states. (b) The phase diagram of the bare-massless case  $m = 0$ , plotted as a function of the filling  $\nu$  and the matter-gauge interaction  $t$ .

$\{2j-1\}$  host quark fermions, with each possessing a fundamental representation  $q = (1, 0) = \{r, g, b\}$  for its color degree of freedom (d.o.f.). Even sites  $\{2j\}$  host antiquark fermions, with an antifundamental representation  $\bar{q} = (0, 1)$ . Via a particle-hole transformation performed on even sites, common to KS Hamiltonians, we convert them to be quarklike ( $q$ ) fermions again, as sketched in Fig. 1(a).

The gauge field (gluon) sublattice, labeled with links  $\{j, j+1\}$ , is defined via its left-hand  $L_{j,j+1}^\mu$  and right-hand  $R_{j,j+1}^\mu$  non-Abelian “electric” field operators [here  $\mu \in \{1, 8\}$  corresponds to the eight generators of the SU(3) group], and by its parallel transporters operators  $U_{j,j+1}^{a,a'}$ , with  $a, b \in \{r, g, b\}$ , which must obey the commutation relations:  $[L_{j,j+1}^\mu, U_{j',j'+1}^{a,a'}] = -\frac{1}{2}\delta_{j,j'}\sum_k \lambda_{a,k}^\mu U_{j,j+1}^{k,a'}$  and  $[R_{j,j+1}^\mu, U_{j',j'+1}^{a,a'}] = \frac{1}{2}\delta_{j,j'}\sum_k U_{j,j+1}^{a,k}\lambda_{k,a'}^\mu$ , where the factors  $\lambda^\mu$  are the eight Gell-Mann matrices. The SU(3) Gauss’s law at every site thus reads  $Q_j^\mu|\Psi_{\text{phys}}\rangle = 0$ ,  $\forall \mu \in \{1, 8\}$  and  $\forall j \in \{1, L\}$ , where

$$Q_j^\mu = R_{j-1,j}^\mu + \sum_{a,a'} \sum_{r,g,b} \frac{\lambda_{a,a'}^\mu}{2} c_{j,a}^\dagger c_{j,a'} + L_{j,j+1}^\mu, \quad (1)$$

unambiguously determining the subspace of physical states  $|\Psi_{\text{phys}}\rangle$ . Equivalently, Gauss’s law requires that each matter field, fused with the gluon to its left (right-hand side) and with the gluon to its right (left-hand side) forms a color singlet (0,0) overall.

The truncated one-dimensional, flavorless, lattice QCD Hamiltonian that we adopt commutes with all of the Gauss law generators  $Q_j^\mu$  and reads

$$\begin{aligned} H_{\text{SU}(3)} = & -\frac{t}{\ell} \sum_{j=1}^{L-1} \sum_{a,a'}^{r,g,b} (c_{j,a}^\dagger U_{j,j+1}^{a,a'} c_{j+1,a'} + \text{H.c.}) \\ & + g\ell \sum_{j=1}^{L-1} (C_{j,j+1}^{(L)} + C_{j,j+1}^{(R)}) \\ & - m \sum_{j=1}^L \sum_a^{r,g,b} (-1)^j c_{j,a}^\dagger c_{j,a}, \end{aligned} \quad (2)$$

where the Dirac fermionic operators  $c_{j,a}^{(\dagger)}$  with  $a \in \{r, g, b\}$  describes the KS matter field and obeys the usual Clifford algebra  $\{c_{j,a}, c_{j',a'}\} = 0$  and  $\{c_{j,a}^\dagger, c_{j',a'}^\dagger\} = \delta_{j,j'}\delta_{a,a'}$ . The operators  $C_{j,j+1}^{(L)} = \sum_{\mu=1}^8 (L_{j,j+1}^\mu)^2$  and  $C_{j,j+1}^{(R)} = \sum_{\mu=1}^8 (R_{j,j+1}^\mu)^2$  are the quadratic Casimir operators, respectively, for the left-hand side and the right-hand side of the gluon at  $\{j, j+1\}$ , and they define the free gluon-field energy term in the Hamiltonian (2). The first line in Eq. (2) represents the coupling between the matter and gauge fields and describes a process of quark-antiquark pair creation/annihilation, which in the staggered fermion language reads as a nearest-neighbor hopping term, while the gluon in the middle link is updated to protect Gauss’s law. The last term in the Hamiltonian represents the bare mass of quarks and antiquarks, and it appears as a staggered chemical potential according to the KS prescription. The straight chemical potential is absent as we run simulations at finite quark density.

In this work, we consider a static cutoff of the gluon field in accordance to its pure energy density. Precisely, we truncate all of the irreducible representations of the gluon field with energy higher than the first nonzero eigenvalue of the Casimir  $C^{(L)}$  and  $C^{(R)}$  (that is,  $\frac{4}{3}$ ). Therefore, the gluon space we are considering is composed by a colorless-colorless  $(0,0) \otimes (0,0)$  state with energy 0, nine quark-antiquark  $q \otimes \bar{q}$  states with energy  $8g\ell/3$ , and nine antiquark-quark  $\bar{q} \otimes q$  states with energy  $8g\ell/3$ , for a total of 19 gluon-field states. In order to increase the cutoff energy [41], it may be possible to follow an approach analogous to Ref. [24] adapted to SU(3); however, we do not perform this study in the present work.

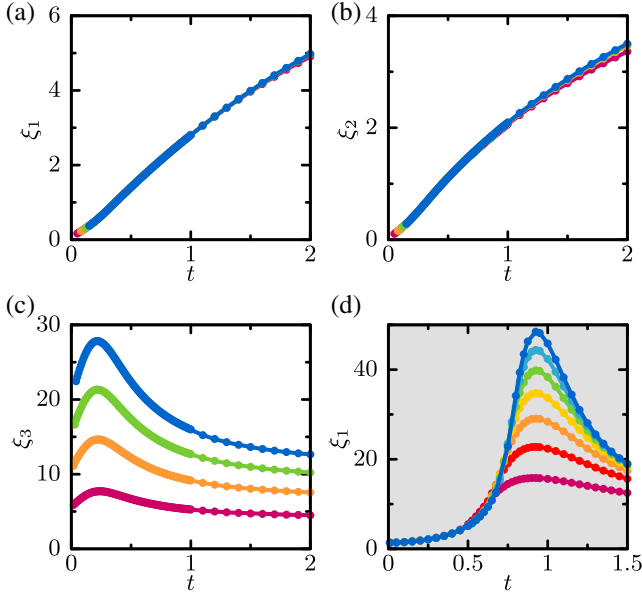


FIG. 2. Correlation lengths  $\xi_\kappa$ , with  $\kappa = 1, 2, 3$ , of the Luttinger liquid order parameters at free-field coupling (a)–(c)  $g > 0$  and, for consistency, check (d)  $g < 0$ . (a)–(c) Here  $\nu = 1$ ,  $m = 0$ , and  $g = 1$ : Only baryonic liquid order emerges. (d) Here  $\nu = -3/2$ ,  $m = 0$ , and  $g = -1$ : A quark liquid appears. System sizes are  $L = 48$  (magenta), 72 (red), 96 (orange), 120 (yellow), 144 (green), 168 (cyan), 192 (blue).

Hereafter, we fix the energy scale by setting  $g = 3/4$  and characterize the ground state  $|\Psi_0\rangle$  of the Hamiltonian (2), as a function of  $t$ ,  $m$  and the fermion filling

$$\nu = L^{-1} \sum_{j=1}^L \sum_a^{r,g,b} c_{j,a}^\dagger c_{j,a}, \quad [H_{\text{SU}(3)}, \nu] = 0, \quad (3)$$

which is a global U(1) symmetry generator. Notice that  $\nu \in [0, 3]$ , and that  $\nu = 3/2$  represents the KS vacuum sector, where there is no matter-antimatter imbalance. The aforementioned truncation allows us to implement *ab initio* manipulations onto the model protecting the SU(3) gauge symmetry, which we carry out in Appendix B, starting from the quantum link formulation of Refs. [27,29]. In order to numerically simulate the quantum system, we use a matrix product state (MPS) description of the many-body quantum state that embeds both the gauge and the global symmetries [10], and we use a time-evolving block decimation (TEBD) algorithm in imaginary time to approximate the ground state  $|\Psi_0\rangle$ . Running simulations with bond-link dimension of the MPS up to  $D \sim 400$  allows us to measure local quantities and correlators with a convergence precision of  $\sim 10^{-6}$ , which is sufficient to characterize the phase properties.

### III. RESULTS: (1) NO DECONFINEMENT

We explore various parameter ranges, searching for phases which exhibit Luttinger liquid (LL) order where

the quasiparticles are, respectively, quarklike, mesonlike, and baryonlike. Single-particle (quarklike) excitations cannot be colorless, so they appear with gluon strings attached. It is possible to define a unique string correlator acting as order parameter of such quarklike LL behavior as

$$\mathcal{C}_{j,j'} = \sum_{a,a'} c_{j,a}^\dagger S_{j,j'}^{a,a'} c_{j',a'}. \quad (4)$$

The string-body operator  $S_{j,j'}^{a,a'}$ , which acts on all of the gluons between sites  $j$  and  $j'$ , satisfies important properties: It transforms covariantly both at its left-hand side and its right-hand side so that  $\mathcal{C}_{j,j'}$  is a gauge-invariant quantity. Moreover,  $S_{j,j'}^{a,a'}$  is unitary, so  $\mathcal{C}_{j,j'}$  can capture long-range order (see Appendix D). Two-particle (mesonlike) excitations, revealing color superconductor order, are captured by  $\mathcal{C}_{j,j'}^2 = (\mathcal{C}_{j,j'})^2$  and also possess a string attached. Finally, the correlator

$$\mathcal{C}_{j,j'}^3 = (\mathcal{C}_{j,j'})^3 = c_{j,r}^\dagger c_{j,g}^\dagger c_{j,b}^\dagger c_{j',b} c_{j',g} c_{j',r} \quad (5)$$

captures a LL order of baryons, or three-particle excitations, which are colorless and thus carry no string. For each of these quasi-long-range order parameters  $\mathcal{C}_{j,j'}^\kappa$  with  $\kappa \in \{1, 2, 3\}$ , we can evaluate the correlation length  $\xi_\kappa$ , which is well approximated by the expression

$$\xi_\kappa = \sqrt{\frac{\sum_{l \neq 0} (|l| - 1)^2 \bar{\mathcal{C}}_l^{(\kappa)}}{\sum_{l \neq 0} \bar{\mathcal{C}}_l^{(\kappa)}}}, \quad (6)$$

where  $\bar{\mathcal{C}}_l^{(\kappa)} = \frac{1}{L-l} \sum_j \langle \Psi_0 | \mathcal{C}_{j,j+l}^\kappa | \Psi_0 \rangle$  are the spatially averaged correlation functions. Compatible with the Mermin-Wagner theorem [42], a LL order of  $\kappa$ -particle excitations is revealed by a diverging correlation length  $\xi_\kappa \rightarrow \infty$  for increasing system sizes  $L \rightarrow \infty$ . We carefully searched different parametric ranges of the model couplings, and we observed that, as long as  $g > 0$  (positive energy densities of the gluon field), only the baryonic Luttinger liquid  $\xi_3$  emerges as a spontaneous quasi-long-range order in the truncated lattice QCD model of Eq. (2). The quarklike and mesonlike order parameter exhibit correlation lengths which never go beyond ten sites [a typical example is shown in Figs. 2(a) and 2(b)] regardless of  $t$ ,  $m$ , and  $\nu$ ; thus such order is not established. Such observation leads to the conclusion that there are no phases (for  $g > 0$ ) with mobile colored quasiparticles, and thus the SU(3) theory under study is strongly confined. This is in contrast to the truncated SU(2) Yang-Mills lattice theory previously studied by some of us [22], which instead exhibited liquid phases with (colored) single-particle excitations. For consistency, we remark that such a strong confinement effect is energetic and not a by-product of symmetry protection. To stress this, we show that, simply by setting a (nonphysical)

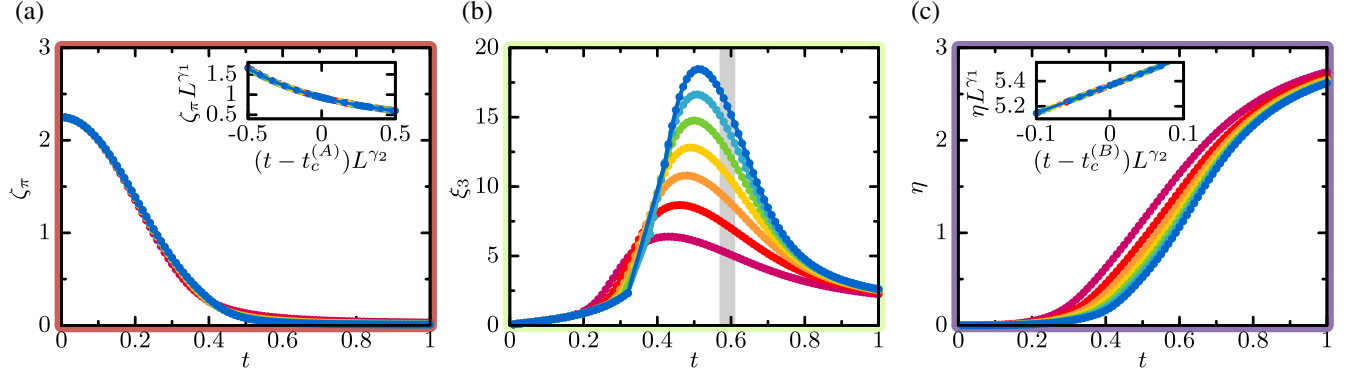


FIG. 3. Order parameters at filling  $\nu = 3/2$  (KS vacuum), as a function of the matter-gauge interaction  $t$ : (a) chiral insulator  $\zeta_\pi$ , (b) baryonic liquid  $\xi_3$ , and (c) dimer insulator  $\eta$ . System sizes are  $L = 48$  (magenta), 72 (red), 96 (orange), 120 (yellow), 144 (green), 168 (cyan), 192 (blue). The shaded region denotes the extrapolated liquid phase  $t_c^{(A)} < t < t_c^{(B)}$ , as determined from finite-size scaling analysis (insets). The panel frames are color coded according to the phase diagram of Fig. 1 and show the order parameter of the corresponding phase.

negative free-field coupling  $g < 0$ , without changing the gluon field truncation, indeed we activate the quark-liquid and meson-liquid orders. This is shown in Fig. 2(d).

#### IV. (2) PHASE DIAGRAM

We explored various parameter regimes after setting  $g = 3/4$ , simulating the ground state of the truncated lattice QCD Hamiltonian for various finite system sizes  $L$ . We estimated the phase properties, reported in Fig. 1(b), by extrapolating the observable quantities at the thermodynamical limit  $L \rightarrow \infty$ . The MPS representation for the variational many-body wave function grants access to the entanglement entropies

$$\mathcal{S}_l = -\text{Tr}[\rho_{1\dots l} \log \rho_{1\dots l}], \quad \text{with } \rho_{1\dots l} = \text{Tr}_{l+1\dots L}[\Psi_0] \langle \Psi_0 |, \quad (7)$$

under any left-right bipartition of the system  $\{1\dots l | l+1\dots L\}$ . We then discriminate between gapped and gapless phases by estimating the central charge  $c$  of the corresponding conformal theory (see Fig. 4), via [43]

$$\mathcal{S}_l \simeq \frac{c}{6} \log(L \sin(\pi l/L)) + S'_l(k_F) + c', \quad (8)$$

where the correction

$$S'_l(k_F) = a' \cos(2k_F(l - L/2)) \sin^{-b'}(\pi l/L) \quad (9)$$

takes into account Fermi oscillations and allows us to access the effective Fermi wave vector  $k_F$ , while  $a'$ ,  $b'$ , and  $c'$  are fitting constants [44,45].

In the bare massless case ( $m = 0$ ), gapped phases are found only in the KS vacuum, which corresponds to filling  $\nu = 3/2$  in the fermion language. A weak-interacting insulator is detected for  $t < t_c^{(A)} \simeq 0.57(1)$ . This phase exhibits chiral order, as it spontaneously breaks the

reflection symmetry  $P$  centered on a link (or equivalently the particle-hole symmetry  $C$ ). Such a phase appears as a charge-density-wave insulator with wave vector  $k = \pi$ , and we characterize it by the order parameter

$$\zeta_\pi = \sqrt{\frac{1}{L(L+1)} \sum_{j \neq j'} e^{i\pi(j-j')} \langle (n_j - \nu)(n_{j'} - \nu) \rangle}. \quad (10)$$

The latter is reported in Fig. 3, where  $n_j = \sum_a^{r,g,b} c_a^\dagger c_a$  is the local density operator. The presence of this phase at low values of the matter-gluon coupling  $t \ll g$  confirms our predictions based on second-order and third-order degenerate perturbation theories in  $t/g$  [46], which are carried out analytically in Appendix E. A second insulating phase exhibiting a different type of order is observed at strong matter-gauge interactions  $t > t_c^{(B)} = 0.61(1)$ . This phase displays a considerable staggerization of entanglement, showing higher entanglement when the bipartition is performed on an odd-even bond, while lower entanglement on an even-odd bond (also shown in Fig. 4). We interpret this effect as the formation of entangled dimers, resembling what is found in the J1-J2 model [47]. If the boundary conditions were periodic, we would expect to see a translationally invariant resonant valence bond state. However, owing to the presence of open boundaries, a specific dimer state is favored, with highly entangled pairs sitting on odd-even  $\{2j-1, 2j\}$  bonds. Ultimately, the bulk, and thus the thermodynamical limit of this phase, will be strongly sensitive to the boundary conditions. As the local order parameter to capture this phase, we adopt the staggered spatial average  $\eta$  of the matter-gauge interaction. Precisely, since we always simulate an even number of sites  $L$ , we set

$$\eta = \left| \frac{2}{L} \sum_{j=1}^{L/2} \langle H_{2j-1,2j}^{\text{inter}} \rangle - \frac{2}{L-2} \sum_{j=1}^{L/2-1} \langle H_{2j,2j+1}^{\text{inter}} \rangle \right|, \quad (11)$$

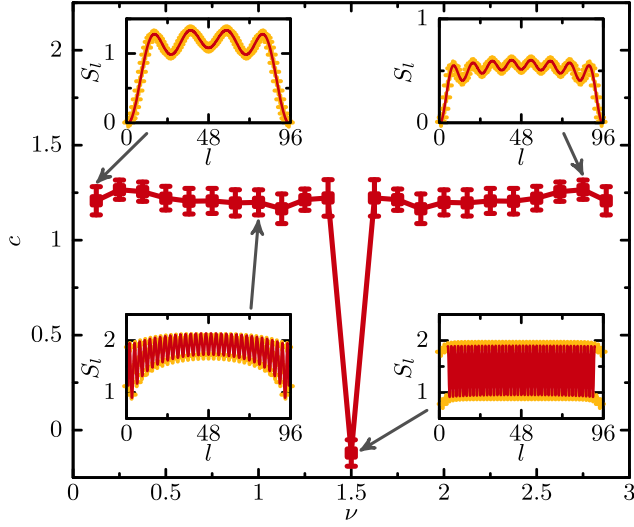


FIG. 4. Central charge  $c$ , as a function of the filling  $\nu$  at  $t = 2.0$ , obtained from fitting the theoretical prediction (see the text) to the entanglement entropy profile  $S_l$ , over partition-size  $l$  at system size  $L = 96$ . The sharp dip at  $\nu = 3/2$  signals the insulating dimer phase. The panels show a few examples of the  $S_l$  profiles and the corresponding fits.

with  $H_{j,j+1}^{\text{inter}} = \sum_{a,a'}^{r,g,b} (c_{j,a}^\dagger U_{j,j+1}^{a,a'} c_{j+1,a'} + \text{H.c.})$ , as the dimer order parameter signaling a spontaneous breaking of the translation by one site, and we observe as it converges to a finite value in the dimer phase (see Fig. 3). We located the critical values  $t_c^{(A)}$  and  $t_c^{(B)}$  via a standard finite-size scaling procedure [48]. We also detected a narrow window  $t_c^{(A)} < t < t_c^{(B)}$ , at filling  $\nu = 3/2$ , where the competition between the two insulating orders actually favors a liquid order: Within this window, we again observe the Luttinger liquid order of baryons, identified by  $\xi_3$  (also shown in Fig. 3). We interpret these results as a vanishing of the mass gap between the lower and upper bands of the baryon conductor. Such a phase, where baryons are effectively massless, emerges in such a narrow interval of the  $t/g$  ratio that we expect it to vanish in the limits of the continuum theory. The phase transition points  $t_c^{(A)}$  and  $t_c^{(B)}$  appear to be compatible with a second-order phase transition, as suggested by the finite-size scaling analysis shown in the Fig. 3 insets. Adopting the scaling function  $\zeta_\pi(t, L) = L^{-\beta_{(A)}/\nu_{(A)}} f_A[(t - t_c^{(A)}) \cdot L^{1/\nu_{(A)}}]$  delivers the critical exponents  $\nu_{(A)} = 2.5(2)$ ,  $\beta_{(A)} = 1.5(1)$ , as reported in Table I. Similarly, the exponents  $\nu_{(B)} = 2.0(2)$ ,  $\beta_{(B)} = 0.6(1)$  result from the scaling function  $\eta(t, L) = L^{-\beta_{(B)}/\nu_{(B)}} f_B[(t - t_c^{(B)}) \cdot L^{1/\nu_{(B)}}]$  with nonuniversal  $f_A$  and  $f_B$ .

For any filling other than the KS vacuum, that is,  $\nu \neq 3/2$ , the system behaves as a band conductor of baryons. Specifically, we observe a divergence with  $L$  of the correlation length  $\xi_3$  related to the Luttinger liquid order

TABLE I. Properties of the critical points, including estimated critical exponents, at zero excess charge density ( $\nu = 3/2$ ) for the massless quark case ( $m = 0$ ), in units of  $g = 3/4$ . Critical points separate the chiral insulator, baryon liquid, and dimer insulator phases.

	$t_c^{(0)}$	$\nu_0$	$\beta_0$	$t < t_c^{(0)}$	$t > t_c^{(0)}$
Crit. point A	0.57(1)	2.5(2)	1.5(1)	Chiral	Liquid
Crit. point B	0.61(1)	2.0(2)	0.6(1)	Liquid	Dimer

of baryons. Similarly, we fit a nonzero central charge  $c \geq 1$  [roughly  $c \simeq 1.3(1)$ ] and a Fermi wave vector  $k_F \simeq \frac{\pi}{3}\nu$ , suggesting that we encounter a single band of weakly interacting, quasifree baryons for  $0 < \nu < 3/2$ , and another band for  $3/2 < \nu < 3$ .

When considering finite bare masses  $m > 0$ , we detect two main changes in the phase diagram. First of all the narrow window of the baryon liquid at the KS vacuum filling  $\nu = 3/2$  disappears completely, and we observe a simple transition between the (induced) chiral insulator and dimer phases. Moreover, we observe the emergence of effectively insulating phases when  $t \ll m$  for any filling  $\nu$ . However, this regime is extremely hard to simulate via imaginary TEBD, and we cannot rule out metastabilities.

### V. (3) BINDING ENERGIES

We also studied the mass gaps, at finite size, of the SU(3) lattice gauge theory. This is possible thanks to our canonical treatment of the particle number symmetry, which allows us to study the system with one or a few excess quarks on top of the KS vacuum, and thus to measure the binding energies between them. This analysis revealed that while each baryon (three quarks) is a strongly bound state, two baryons (six quarks) weakly repel each other. This suggests that (flavorless) lattice QCD in 1D disfavors the creation of multibaryon bound states, such as atomic nuclei, in sharp contrast with QCD in three dimensions (see the appendixes for more details).

### VI. CONCLUSIONS

We simulate in this paper the equilibrium properties of a compact one-dimensional flavorless lattice QCD: The theory is strongly confined, as it exhibits only colorless quasiparticles. Only at the Kogut-Susskind vacuum ( $\nu = 3/2$ ) do insulating phases appear: Precisely, we observe a competition between a chiral and a dimer phase, separated by a small gapless window only at zero bare mass. Moreover, in this framework, baryons do not form aggregates. Our approach shows once again the power of a tensor network for treating nonperturbatively lattice gauge theories in low dimensions, while exactly capturing the

gauge symmetry content, even when it is a complex non-Abelian structure such as the SU(3) group.

### ACKNOWLEDGMENTS

We warmly thank A. Celi, K. Jansen, U.-J. Wiese, and P. Zoller for the stimulating private discussions. The authors kindly acknowledge financial support from the EU via ERC Synergy Grant UQUAM, the QuantERA project QTFLAG, and the Quantum Flagship PASQUANS, from the Italian PRIN 2017, from the Baden-Württemberg Stiftung via Eliteprogramm for PostDocs, from the Carl-Zeiss-Stiftung via Nachwuchsförderprogramm, from the Austrian Research Promotion Agency (FFG) via QFTE project AutomatiQ, and from the DFG via the TWITTER project.

### APPENDIX A: QUANTUM LINK MODEL DERIVATION

In this section, we discuss how to explicitly obtain the 19-state truncated SU(3) lattice gauge model under our study from a quantum link model perspective, following the mapping discussed in Refs. [27,29]. This pathway allows us to easily compute all of the relevant matrix elements for the various effective operators of the many-body model so that we can export them on a numerical simulation platform (see Appendix B). In this paradigm, each gauge field d.o.f.  $\{j, j+1\}$  is replaced by a pair of quark-colored fermionic modes, or “rishons,”  $\{j, L\}$  and  $\{j+1, R\}$ . Hence, the substitutions

$$\begin{aligned} U_{j,j+1}^{a,a'} &\rightarrow \psi_{j,L,a} \psi_{j+1,R,a'}^\dagger, \\ L_{j,j+1}^\mu &\rightarrow \frac{1}{2} \sum_{a,a'} \psi_{j,L,a}^\dagger \lambda_{a,a'}^\mu \psi_{j,L,a}, \quad \text{and} \\ R_{j,j+1}^\mu &\rightarrow \frac{1}{2} \sum_{a,a'} \psi_{j+1,R,a}^\dagger \lambda_{a,a'}^\mu \psi_{j+1,R,a}, \end{aligned} \quad (\text{A1})$$

provide the correct commutation relations between  $U_{j,j+1}^{a,a'}$  and  $L_{j,j+1}^\mu$  and  $R_{j,j+1}^\mu$ , respectively. Such splitting generates an Abelian link symmetry [49] as a by-product, generated by  $\mathcal{N}_{j,j+1} = n_{j,L} + n_{j+1,R} = \sum_a \psi_{j,L,a}^\dagger \psi_{j,L,a} + \sum_a \psi_{j+1,R,a}^\dagger \psi_{j+1,R,a}$ . Specifically, we work in the symmetry sector  $\mathcal{N}_{j,j+1} |\Psi_{\text{phys}}\rangle = 3 |\Psi_{\text{phys}}\rangle$ , where the representation of a left rishon mode is always linked to its dual representation in the right rishon mode. This produces automatically a 20-dimensional gluon-field space which contains the desired 19-state truncated space. Precisely, the two states with  $n_{j,L} = 0$  and  $n_{j,L} = 3$  transform both as colorless-colorless  $(0,0) \otimes (0,0)$  states, while the nine states with  $n_{j,L} = 1$  correspond to the quark-antiquark  $q \otimes \bar{q}$  states, and finally the nine states  $n_{j,L} = 2$  correspond to the antiquark-quark states  $\bar{q} \otimes q$ . Under these

considerations, we can formally rewrite the (bare) free-field term of the truncated lattice QCD Hamiltonian as

$$\begin{aligned} H_{\text{ff}} &= \frac{3}{8} g_0 \sum_{j=1}^{L-1} (C_{j,j+1}^{(L)} + C_{j,j+1}^{(R)}) \\ &= \frac{g_0}{4} \sum_{j=1}^{L-1} n_{j,L} (3 - n_{j,L}) + n_{j+1,R} (3 - n_{j+1,R}), \end{aligned} \quad (\text{A2})$$

where now the two colorless-colorless states have energy 0, and the other 18 states have energy  $g_0$ .

In addition to the aforementioned splitting, quantum link formulations of gauge theories add an extra term in the Hamiltonian whose purpose is to break the artificial U(1) symmetry, generated by  $\mathcal{Q}_j = n_{j,R} + \sum_a c_{j,a}^\dagger c_{j,a} + n_{j,L}$ . This symmetry is unwanted, as it changes the gauge transformations from an SU(3) group into a U(3) group. The dynamical breaking terms thus typically takes the form

$$\begin{aligned} H_{\text{break}} &= -\varepsilon \sum_{j=1}^{L-1} (\psi_{j,L,r}^\dagger \psi_{j,L,g} \psi_{j,L,b}^\dagger \\ &\quad \times \psi_{j+1,R,b} \psi_{j+1,R,g} \psi_{j+1,R,r} + \text{H.c.}), \end{aligned} \quad (\text{A3})$$

also acting solely on the gauge d.o.f. and rightfully preserving all of the other symmetries. This extra component also has the merit of breaking the energy degeneracy of the two colorless-colorless gluon states, producing one reflection-symmetric state at energy  $-\varepsilon$  and one reflection-antisymmetric state at energy  $+\varepsilon$ . We can now recover exactly the desired 19-state representation by energetically eliminating one of these two states, i.e., by setting  $g_0 = (\frac{8}{3} g\ell - \varepsilon)$  and  $\varepsilon \gg g\ell$ . As we approach  $\varepsilon \rightarrow +\infty$ , the original free-field Hamiltonian is recovered (apart from a constant).

### APPENDIX B: COMPOSITE-SITE GAUGE-INVARIANT BASIS AND GAUGE GROUP REDUCTION

In the following sections, we perform some analytic manipulations of the truncated lattice QCD model in order to simplify the many-body quantum problem in a format which is fit for numerical simulation. First of all we construct all of the possible gauge-invariant quasilocal states and show that it is possible to express them in a color-transparent occupation basis. We will then be able to evaluate all of the matrix elements of the truncated lattice QCD Hamiltonian on this basis.

To represent the matter states, we write sites  $|0\rangle$  as the bare staggered vacuum (empty matter, full antimatter), then the singly occupied states  $|r\rangle = c_r^\dagger |0\rangle$ ,  $|g\rangle = c_g^\dagger |0\rangle$ , and  $|b\rangle = c_b^\dagger |0\rangle$  (red, green, and blue, respectively), followed by the doubly occupied states  $|y\rangle = c_r^\dagger c_g^\dagger |0\rangle$ ,  $|c\rangle = c_g^\dagger c_b^\dagger |0\rangle$ ,

and  $|m\rangle = -c_r^\dagger c_b^\dagger |0\rangle$  (cyan, yellow, and magenta), and finally the triply occupied state  $|3\rangle = c_r^\dagger c_g^\dagger c_b^\dagger |0\rangle$ .

To represent the rishon sites (either the left or right side of a gluon field), we similarly adopt  $|r\rangle, |g\rangle, |b\rangle$  to characterize the quarklike  $q$  subspace,  $|y\rangle, |c\rangle, |m\rangle$  to characterize the antiquarklike  $\bar{q}$  subspace, and  $|0\rangle$  to represent the colorless (0,0) subspace.

We can now list the gauge-invariant states of the quasilocal space, which includes a matter site  $j$ , the right rishon space  $R$  of the gluon to its left  $\{j-1, j\}$ , and the left rishon space  $L$  of the gluon to its right  $\{j, j+1\}$ :

$$\begin{aligned}
 &|0, 0, 0\rangle, \\
 &|1, 0, 2\rangle := \frac{1}{\sqrt{3}}(|r, 0, c\rangle + |g, 0, m\rangle + |b, 0, y\rangle), \\
 &|2, 0, 1\rangle := \frac{1}{\sqrt{3}}(|c, 0, r\rangle + |m, 0, g\rangle + |y, 0, b\rangle), \\
 &|0, 1, 2\rangle := \frac{1}{\sqrt{3}}(|0, r, c\rangle + |0, g, m\rangle + |0, b, y\rangle), \\
 &|1, 1, 1\rangle := \frac{1}{\sqrt{6}}(|r, g, b\rangle + |g, b, r\rangle + |b, r, g\rangle + \\
 &\quad - |g, r, b\rangle - |r, b, g\rangle - |b, r, g\rangle), \\
 &|2, 1, 0\rangle := \frac{1}{\sqrt{3}}(|c, r, 0\rangle + |m, g, 0\rangle + |y, b, 0\rangle), \\
 &|1, 2, 0\rangle := \frac{1}{\sqrt{3}}(|r, c, 0\rangle + |g, m, 0\rangle + |b, y, 0\rangle), \\
 &|2, 2, 2\rangle := \frac{1}{\sqrt{6}}(|c, y, m\rangle + |y, m, c\rangle + |m, c, y\rangle + \\
 &\quad - |c, m, y\rangle - |m, y, c\rangle - |y, c, m\rangle), \\
 &|0, 3, 0\rangle, \\
 &|1, 3, 2\rangle := \frac{1}{\sqrt{3}}(|r, 3, c\rangle + |g, 3, m\rangle + |b, 3, y\rangle), \\
 &|2, 3, 1\rangle := \frac{1}{\sqrt{3}}(|c, 3, r\rangle + |m, 3, g\rangle + |y, 3, b\rangle), \quad (\text{B1})
 \end{aligned}$$

for a total of 12 composite-site gauge-invariant states. It is immediately visible that such an occupation basis expansion  $|\chi_R, \chi_M, \chi_L\rangle$ , with  $\chi_R, \chi_L \in \{0, 1, 2\}$  and  $\chi_M \in \{0, 1, 2, 3\}$ , bears no further color ambiguity once Gauss's law is set, so it can be comfortably used for numerical simulations. We remark that the  $\chi_{R/L}$  basis notation differs from the  $n_{R/L}$  basis notation in the sense that one the two colorless-colorless gluon basis states has already been removed (see Appendix A).

In this basis, it is straightforward to see that the non-Abelian SU(3) Gauss law can be recast, within the truncated space, as an Abelian  $\mathbb{Z}_3$  Gauss law, where  $\mathbb{Z}_3$  is the Abelian cyclic group with three elements ( $g, g^2 = g^{-1}$ , and  $g^3 = 1$ ), the center of SU(3). Namely, let us define at

every composite site  $j$  the unitary operator  $\Gamma|\chi_R, \chi_M, \chi_L\rangle = e^{\frac{2i\pi}{3}(\chi_R + \chi_M + \chi_L)}|\chi_R, \chi_M, \chi_L\rangle$ . The transformation  $\Gamma$  clearly forms a  $\mathbb{Z}_3$  group since  $\Gamma^3 = \mathbb{1}$ . In the truncated space, the Gauss law of Eq. (1) can be cast simply in terms of the  $\Gamma$  operators and reads  $\Gamma_j|\Psi_{\text{phys}}\rangle = |\Psi_{\text{phys}}\rangle \forall j \in \{1, L\}$ . In simple terms, the reduced Gauss law requires that, at every site  $j$ ,  $\chi_R + \chi_M + \chi_L$  modulo 3 is equal to zero, which is indeed a  $\mathbb{Z}_3$  symmetry constraint. As a final remark, we also point out that the link symmetry constraint, enforcing the fact that the left and right representations of a bond are mutually dual, can be similarly cast in a  $\mathbb{Z}_3$  fashion since it can be written as  $(\chi_{j,L} + \chi_{j+1,R}) \% 3 = 0$ .

### APPENDIX C: MATRIX ELEMENTS OF THE HAMILTONIAN

In this section, we derive the matrix elements for the operators that appear in the Hamiltonian (1) when expressed in the composite-site gauge-invariant basis we constructed in Appendix B. These effective operators directly follow from the quantum link modelization (see Appendix A), from which we projected away the reflection-antisymmetric colorless-colorless state

$$\begin{aligned}
 |\infty\rangle_{j,j+1} = &\frac{1}{\sqrt{2}}(\psi_{j,L,r}^\dagger \psi_{j,L,g}^\dagger \psi_{j,L,b}^\dagger + \\
 &+ \psi_{j+1,R,r}^\dagger \psi_{j+1,R,g}^\dagger \psi_{j+1,R,b}^\dagger)|\Omega\rangle, \quad (\text{C1})
 \end{aligned}$$

where  $|\Omega\rangle$  is the particle vacuum ("full antimatter universe" in KS language). The effective 19-gluon-state Hamiltonian is then obtained from the 20-gluon-state one in the first-order perturbation theory sense  $H^{(1)} = PHP$ , where the projector  $P = \bigotimes_j^{L-1} (\mathbb{1} - |\infty\rangle\langle\infty|)_{j,j+1}$  removes the unwanted colorless-colorless state from each link.

According to this prescription, the various components of the truncated Hamiltonian (2) can be expressed as simple operators in the color-transparent occupation basis: The free-field term reads

$$H_{\text{ff}}^{(1)} = \frac{2g\ell}{3} \sum_{j=1}^{L-1} \chi_{j,L}(3 - \chi_{j,L}) + \chi_{j+1,R}(3 - \chi_{j+1,R}), \quad (\text{C2})$$

while the bare mass term reads

$$H_{\text{bm}}^{(1)} = m \sum_{j=1}^{L-1} (-1)^j \chi_{j,M}, \quad (\text{C3})$$

where now  $\chi$  are meant as operators. The matter-gauge interaction term of the Hamiltonian can be comfortably written as  $H_{\text{inter}}^{(1)} = -\frac{t}{\ell} \sum_{j=1}^{L-1} A_j^{L\dagger} A_{j+1}^R + \text{H.c.}$ , where the single composite-site operators  $A^{L\dagger}$  and  $A^R$  are

$$\begin{aligned}
A^{L\dagger} = & \sqrt[4]{\frac{9}{2}}|0, 3, 0\rangle\langle 0, 2, 1| + 2|0, 2, 1\rangle\langle 0, 1, 2| \\
& + \sqrt[4]{\frac{9}{2}}|0, 1, 2\rangle\langle 0, 0, 0| + \sqrt[4]{2}|1, 2, 0\rangle\langle 1, 1, 1| \\
& + \sqrt{2}|1, 1, 1\rangle\langle 1, 0, 2| + \sqrt[4]{\frac{1}{2}}|1, 3, 2\rangle\langle 1, 2, 0| \\
& + \sqrt{2}|2, 3, 1\rangle\langle 2, 2, 2| + \sqrt[4]{2}|2, 2, 2\rangle\langle 2, 1, 0| \\
& + \sqrt[4]{\frac{1}{2}}|2, 1, 0\rangle\langle 2, 0, 1| \tag{C4}
\end{aligned}$$

and

$$\begin{aligned}
A^R = & \sqrt[4]{\frac{9}{2}}|0, 0, 0\rangle\langle 2, 1, 0| + 2|2, 1, 0\rangle\langle 1, 2, 0| \\
& + \sqrt[4]{\frac{9}{2}}|1, 2, 0\rangle\langle 0, 3, 0| + \sqrt{2}|2, 0, 1\rangle\langle 1, 1, 1| \\
& + \sqrt[4]{2}|1, 1, 1\rangle\langle 0, 2, 1| + \sqrt[4]{\frac{1}{2}}|0, 2, 1\rangle\langle 2, 3, 1| \\
& + \sqrt[4]{2}|0, 1, 2\rangle\langle 2, 2, 2| + \sqrt{2}|2, 2, 2\rangle\langle 1, 3, 2| \\
& + \sqrt[4]{\frac{1}{2}}|1, 0, 2\rangle\langle 0, 1, 2|, \tag{C5}
\end{aligned}$$

respectively. These matrices can be comfortably used in numerical simulations, such as the imaginary TEBD we employed to obtain our results.

#### APPENDIX D: STRING OPERATORS FOR FLUID CORRELATION FUNCTIONS

In this paragraph, we construct explicitly the unitary string operator  $S_{j,j'}^{a,a'}$ , which we use in the evaluation of single-quark fluidity correlation matrix  $\langle C_{j,j'} \rangle$ . As mentioned in the paper, we require it to be a unitary space propagator (in the truncated model) and to transform covariantly so that the correlator  $C_{j,j'} = \sum_{a,a'} c_{j,a}^\dagger S_{j,j'}^{a,a'} c_{j',a'}$  preserves Gauss's law at every site.

For such construction, it is extremely convenient to work in the occupation basis  $|\chi_R, \chi_M, \chi_L\rangle$ , on which Gauss's law is expressed as the  $\mathbb{Z}_3$  symmetry  $[(\chi_{j,R} + \chi_{j,M} + \chi_{j,L}) \% 3] |\Psi_{\text{phys}}\rangle = 0$ , and the link symmetry as  $[(\chi_{j,L} + \chi_{j+1,R}) \% 3] |\Psi_{\text{phys}}\rangle = 0$ .

In this language, the correlators are simply expressed as

$$C_{j,j'} = T_j^{M\dagger} \left( \prod_{k=j}^{j'-1} B_{k,k+1} \right) T_{j'}^M, \tag{D1}$$

where the order of the operators is not relevant as they all commute. In fact, the ‘‘tail’’ operators  $T^M$  act only on matter modes and retain some freedom: For simplicity, we chose them to be

$$T_M = |0\rangle\langle 1| + |1\rangle\langle 2| + |2\rangle\langle 3|. \tag{D2}$$

Each ‘‘body’’ operator  $B_{j,j+1}$  instead acts only on rishon modes  $\{j, L\}$  and  $\{j+1, R\}$ . In order to preserve all link and Gauss symmetries, they must be of the following form (apart from phase factors),

$$B_{j,j+1} = |0, 0\rangle\langle 1, 2| + |1, 2\rangle\langle 2, 1| + |2, 1\rangle\langle 0, 0|, \tag{D3}$$

which is a cyclic operator  $B^3 = 1$ . We employ those string operators to investigate the presence of various Luttinger liquid orders—respectively, liquid phases where the quasiparticles are quarklike ( $C_{j,j'}$ ), mesonlike ( $C_{j,j'}^2$ ), or baryonlike ( $C_{j,j'}^3$ ).

#### APPENDIX E: PERTURBATION THEORY AT $t \ll g$

In this section, we will derive an effective Hamiltonian, corresponding to the second-order degenerate perturbation theory in  $t$ , acting upon the ground space of the free-field Hamiltonian, to better understand the phase diagram in the limit  $t \ll g$  (after setting  $\ell = 1$ ). First of all we identify the ground space of the free-field Hamiltonian: Using the free-field term in the form of Eq. (C2), we immediately see that every link  $\{j, j+1\}$  must be in the colorless-colorless state  $|0, 0\rangle$ , the kernel of the positive Casimir operators  $C_j^{(L)}$  and  $C_{j+1}^{(R)}$ . Owing to the reduced  $\mathbb{Z}_3$  Gauss law, and having set the leftmost boundary to be colorless, we conclude that each matter site can be in only either an empty state or a triply occupied (baryon) state; thus either  $|0\rangle$  or  $|3\rangle = c_r^\dagger c_g^\dagger c_b^\dagger |0\rangle$ . The ground space of the free-field Hamiltonian is thus equivalent to a 1D lattice of spinless fermions, given that baryon operators  $b^\dagger = c_r^\dagger c_g^\dagger c_b^\dagger$  mutually anticommute as Dirac fermions.

First-order perturbation theory on this effective subspace provides no change since every matrix element of the matter-field interaction Hamiltonian restricted to this subspace is identically zero:  $PH_{\text{inter}}^{(1)}P = 0$ , where  $P$  is the projector onto the subspace. At this point, we can consider second-order processes on each pair of neighboring sites since the free-field Hamiltonian is fully local and the matter-field interaction acts on nearest neighbors [46]. States of the type  $|0, 0, 0\rangle_j |0, 0, 0\rangle_{j+1}$  and  $|0, 3, 0\rangle_j |0, 3, 0\rangle_{j+1}$  allow for no second-order processes. On the other hand, the state  $|0, 0, 0\rangle_j |0, 3, 0\rangle_{j+1}$  can virtually excite to the state  $|0, 1, 2\rangle_j |1, 2, 0\rangle_{j+1}$  via  $H_{\text{inter}}^{(1)}$ , with amplitude  $-\frac{3\sqrt{2}}{2}t$ . In turn, the state  $|0, 1, 2\rangle_j |1, 2, 0\rangle_{j+1}$ , after freely propagating with inverse excitation energy  $(H_{\text{ff}}^{(1)} - E_0)^{-1}$  equal to  $\frac{3}{8g}$ , can go back to the subspace in a single  $H_{\text{inter}}^{(1)}$  excitation only by returning to  $|0, 0, 0\rangle_j |0, 3, 0\rangle_{j+1}$ . Using the previous argument, we

conclude that the state  $|0, 0, 0\rangle_j |0, 3, 0\rangle_{j+1}$  acquires a perturbed energy equal to  $-27t^2/(16g)$ . By left-right reflection symmetry, the state  $|0, 3, 0\rangle_j |0, 0, 0\rangle_{j+1}$  acquires the same energy. The effective Hamiltonian  $H^{(2)} = PH_{\text{inter}}^{(1)}(H_{\text{ff}}^{(1)} - E_0)^{-1}H_{\text{inter}}^{(1)}P$  deriving from the second-order perturbation theory in  $t$  will thus read

$$H^{(2)} = +\frac{27t^2}{32g} \sum_j^{L-1} \sigma_j^z \sigma_{j+1}^z - \frac{3m}{2} \sum_{j=1}^L (-1)^j \sigma_j^z, \quad (\text{E1})$$

where we reintroduced the bare mass term (which is exact since it commutes with the free-field Hamiltonian), and where we recast the baryon lattice into a spin lattice via the Jordan-Wigner transformation, simply using  $\sigma_j^z = 2b_j^\dagger b_j - 1$ . The additional parameter that we control in our simulations, the particle filling  $\nu$ , is equivalent to  $\nu = \frac{3}{2} + \frac{1}{L} \sum_j \sigma_j^z$  in this language.

In the bare-massless case, such a ZZ Hamiltonian is gapped at the filling sector  $\nu = 3/2$  (corresponding to zero magnetization), and it has a doubly degenerate ground state, corresponding to the two Z-aligned antiferromagnets. This degeneracy spontaneously breaks the full spin-flip (particle-hole) symmetry, and establishes the chiral order parameter  $\zeta_\pi$ , which indeed we observed numerically for  $t \leq t_c^{(A)}g$ .

For other particle fillings  $\nu$ , at zero bare mass  $m$ , the effective second-order Hamiltonian  $H^{(2)}$  has an extensive degeneracy of the ground space; thus to better understand the phases, we find that at  $t \ll g$ , it is helpful to consider additionally the third order of the perturbation theory. Since  $PH_{\text{inter}}^{(1)}P = 0$ , the only relevant contribution to the third-order effective Hamiltonian is of the form  $H^{(3)} = PH_{\text{inter}}^{(1)}(H_{\text{ff}}^{(1)} - E_0)^{-1}H_{\text{inter}}^{(1)}(H_{\text{ff}}^{(1)} - E_0)^{-1}H_{\text{inter}}^{(1)}P$ , which leads to

$$\begin{aligned} H^{(3)} &= \frac{81t^3}{32g^2} \sum_j^{L-1} b_j^\dagger b_{j+1} + \text{H.c.} \\ &= \frac{81t^3}{32g^2} \sum_j^{L-1} \sigma_j^+ \sigma_{j+1}^- + \sigma_j^- \sigma_{j+1}^+, \end{aligned} \quad (\text{E2})$$

where again we used the Jordan-Wigner transformation. This effective tight-binding Hamiltonian for fermions produces a finite bandwidth for the free-fermion modes, which in turn will produce a fermionic band-conducting phase for fillings  $\nu \neq 3/2$ . Nevertheless, activating the bare mass  $m \neq 0$  dampens the hopping processes, resulting again in an emergent insulating behavior.

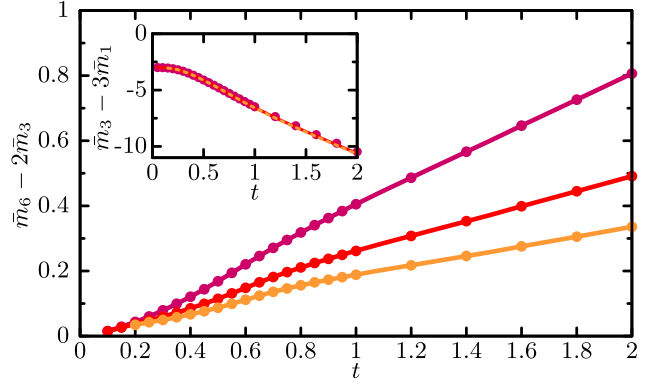


FIG. 5. Binding energy  $\bar{m}_6 - 2\bar{m}_3$  of two baryons, as a function of  $t$ , for system sizes  $L = 48$  (magenta),  $72$  (red),  $96$  (orange). (Inset) Binding energy  $\bar{m}_3 - 3\bar{m}_1$  of the three quarks forming a single baryon. The sizes  $L$  are color coded as in the main panel.

## APPENDIX F: BINDING ENERGIES

Here we report the estimation of binding energies of few-body, eventually bound, states, based on the measurement of the mass gaps  $\bar{m}_k$  of  $k$  quarks on top of the dressed vacuum  $\nu = \frac{3}{2}$ . To do so, we numerically simulate the ground state energies  $E(\nu)$  for  $\nu = \frac{3}{2} + k/L$ , with excess quark number  $k$  from the set  $k \in \{0, 1, 3, 6\}$ . The corresponding  $k$ -quark mass gap (that is, the chemical potential for  $k$  additional quarks) is thus  $\bar{m}_k = E(\frac{3}{2} + k/L) - E(\frac{3}{2})$ . We can then compare the various  $\bar{m}_k$  to estimate the binding energies of composite particles.

We first consider the binding energy of a baryon, formed by three quarks. Its binding energy,  $\bar{m}_3 - 3\bar{m}_1$ , is reported in Fig. 5 (inset) as a function of  $t$ , for zero bare mass  $m$ . We observe not only that this binding energy is negative, but also that it is insensitive to the system size. This suggests that the three quarks indeed form a bound state, which has finite size in the relative coordinates with respect to the center of mass, once again corroborating the strong confinement of quarks [4] in our model.

Secondly, we consider the binding energy of a deuteron, i.e., a state formed by two baryons, or six quarks; hence,  $k = 6$ . The main panel of Fig. 5 shows that the deuteron binding energy  $\bar{m}_6 - 2\bar{m}_3$  is positive, revealing that the two baryons do not form a bound state, while instead they repel each other. Moreover, we observe that such repulsion energy decreases with the system size. We consider this a signature that the effective interaction energy scales with the distance of the two baryons: As the size  $L$  increases, they have more space to sit far apart, and the resulting interaction energy decreases. The repulsion between baryons is thus somewhat “weak” compared to the color confinement effects.

- [1] J. Möller and Y. Schroder, *Nucl. Phys. B, Proc. Suppl.* **205–206**, 218 (2010).
- [2] M. A. Halasz, A. D. Jackson, R. E. Shrock, M. A. Stephanov, and J. J. M. Verbaarschot, *Phys. Rev. D* **58**, 096007 (1998).
- [3] M. Stephanov, *Proc. Sci., LAT2006* (2006) 024.
- [4] K. G. Wilson, *Phys. Rev. D* **10**, 2445 (1974).
- [5] J. Kogut and L. Susskind, *Phys. Rev. D* **11**, 395 (1975).
- [6] J. Schwinger, *Phys. Rev.* **128**, 2425 (1962).
- [7] C. Hamer, Z. Weihong, and J. Oitmaa, *Phys. Rev. D* **56**, 55 (1997).
- [8] M. Troyer and U.-J. Wiese, *Phys. Rev. Lett.* **94**, 170201 (2005).
- [9] T. Byrnes, P. Sriganesh, R. Bursill, and C. Hamer, *Phys. Rev. D* **66**, 013002 (2002).
- [10] P. Silvi, E. Rico, T. Calarco, and S. Montangero, *New J. Phys.* **16**, 103015 (2014).
- [11] L. Tagliacozzo, A. Celi, and M. Lewenstein, *Phys. Rev. X* **4**, 041024 (2014).
- [12] M. C. Bañuls, K. Cichy, J. I. Cirac, K. Jansen, and S. Kühn, *Proc. Sci., LATTICE2018* (2018) 022.
- [13] L. Tagliacozzo and G. Vidal, *Phys. Rev. B* **83**, 115127 (2011).
- [14] E. Rico, T. Pichler, M. Dalmonte, P. Zoller, and S. Montangero, *Phys. Rev. Lett.* **112**, 201601 (2014).
- [15] M. C. Bañuls, K. Cichy, J. I. Cirac, K. Jansen, and H. Saito, *Proc. Sci., LATTICE2013* (2013) 332.
- [16] M. C. Bañuls, K. Cichy, J. I. Cirac, K. Jansen, and S. Kühn, *Phys. Rev. Lett.* **118**, 071601 (2017).
- [17] B. Buyens, J. Haegeman, K. Van Acoleyen, H. Verschelde, and F. Verstraete, *Phys. Rev. Lett.* **113**, 091601 (2014).
- [18] M. Bañuls, K. Cichy, J. Cirac, and K. Jansen, *J. High Energy Phys.* **11** (2013) 158.
- [19] B. Buyens, K. Van Acoleyen, J. Haegeman, and F. Verstraete, *Proc. Sci., LATTICE2014* (2014) 308.
- [20] B. Buyens, J. Haegeman, H. Verschelde, F. Verstraete, and K. Van Acoleyen, *Phys. Rev. X* **6**, 041040 (2016).
- [21] B. Buyens, J. Haegeman, F. Hebenstreit, F. Verstraete, and K. Van Acoleyen, *Phys. Rev. D* **96**, 114501 (2017).
- [22] P. Silvi, E. Rico, M. Dalmonte, F. Tschirsich, and S. Montangero, *Quantum* **1**, 9 (2017).
- [23] S. Kühn, E. Zohar, J. I. Cirac, and M. C. Bañuls, *J. High Energy Phys.* **07** (2015) 130.
- [24] M. C. Bañuls, K. Cichy, J. I. Cirac, K. Jansen, and S. Kühn, *Phys. Rev. X* **7**, 041046 (2017).
- [25] D. Horn, *Phys. Lett.* **100B**, 149 (1981).
- [26] P. Orland and D. Rohrlich, *Nucl. Phys.* **B338**, 647 (1990).
- [27] R. Brower, S. Chandrasekharan, and U.-J. Wiese, *Phys. Rev. D* **60**, 094502 (1999).
- [28] E. Zohar and M. Burrello, *Phys. Rev. D* **91**, 054506 (2015).
- [29] S. Chandrasekharan and U.-J. Wiese, *Nucl. Phys.* **B492**, 455 (1997).
- [30] S. P. Jordan, K. S. M. Lee, and J. Preskill, *Science* **336**, 1130 (2012).
- [31] D. Banerjee, M. Bögli, M. Dalmonte, E. Rico, P. Stebler, U.-J. Wiese, and P. Zoller, *Phys. Rev. Lett.* **110**, 125303 (2013).
- [32] L. Tagliacozzo, A. Celi, A. Zamora, and M. Lewenstein, *Ann. Phys. (Amsterdam)* **330**, 160 (2013).
- [33] L. Tagliacozzo, A. Celi, P. Orland, M. W. Mitchell, and M. Lewenstein, *Nat. Commun.* **4**, 2615 (2013).
- [34] E. Zohar, A. Farace, B. Reznik, and J. I. Cirac, *Phys. Rev. A* **95**, 023604 (2017).
- [35] E. A. Martinez, C. A. Muschik, P. Schindler, D. Nigg, A. Erhard, M. Heyl, P. Hauke, M. Dalmonte, T. Monz, P. Zoller, and R. Blatt, *Nature (London)* **534**, 516 (2016).
- [36] O. Dutta, L. Tagliacozzo, M. Lewenstein, and J. Zakrzewski, *Phys. Rev. A* **95**, 053608 (2017).
- [37] N. Klco, E. F. Dumitrescu, A. J. McCaskey, T. D. Morris, R. C. Pooser, M. Sanz, E. Solano, P. Lougovski, and M. J. Savage, *Phys. Rev. A* **98**, 032331 (2018).
- [38] C. Kokail, C. Maier, R. van Bijnen, T. Brydges, M. K. Joshi, P. Jurcevic, C. A. Muschik, P. Silvi, R. Blatt, C. F. Roos *et al.*, *Nature (London)* **569**, 355 (2019).
- [39] H.-H. Lu, N. Klco, J. M. Lukens, T. D. Morris, A. Bansal, A. Ekström, G. Hagen, T. Papenbrock, A. M. Weiner, M. J. Savage *et al.*, *Phys. Rev. A* **100**, 012320 (2019).
- [40] J. Kogut, *Rev. Mod. Phys.* **51**, 659 (1979).
- [41] B. Buyens, S. Montangero, J. Haegeman, F. Verstraete, and K. Van Acoleyen, *Phys. Rev. D* **95**, 094509 (2017).
- [42] N. D. Mermin and H. Wagner, *Phys. Rev. Lett.* **17**, 1133 (1966).
- [43] P. Calabrese and J. Cardy, *J. Stat. Mech.* (2004) P06002.
- [44] P. Calabrese, M. Campostrini, F. Essler, and B. Nienhuis, *Phys. Rev. Lett.* **104**, 095701 (2010).
- [45] P. Calabrese, J. Cardy, and I. Peschel, *J. Stat. Mech.* (2010) P09003.
- [46] S. Bravyi, D. P. DiVincenzo, and D. Loss, *Ann. Phys. (Amsterdam)* **326**, 2793 (2011).
- [47] F. D. M. Haldane, *Phys. Rev. B* **25**, 4925 (1982).
- [48] M. E. Fisher and M. N. Barber, *Phys. Rev. Lett.* **28**, 1516 (1972).
- [49] P. Silvi, E. Rico, T. Calarco, and S. Montangero, *New J. Phys.* **16**, 103015 (2014).